Phase separation in deuterated polycarbonate/poly(methylmethacrylate) blend near glass transition temperature

5 AUTHORS, INCLUDING:

Hiroshi Jinnai
Tohoku University

234 PUBLICATIONS   **4,233** CITATIONS

SEE PROFILE

Tetsuo Hashimoto
Niigata University

186 PUBLICATIONS   **1,478** CITATIONS

SEE PROFILE

Phase separation in deuterated polycarbonate/poly(methylmethacrylate) blend near glass transition temperature

M. Motowoka,[a] H. Jinnai, and T. Hashimoto
Department of Polymer Chemistry, Kyoto University, Kyoto, 606 Japan

Y. Qiu[b] and C. C. Han
Polymers Division, National Institute of Standards & Technology, Gaithersburg, Maryland 20899

Early stage of spinodal decomposition kinetics of deuterated polycarbonate/poly(methylmethacrylate) blend has been studied by the time resolved small angle neutron scattering measurements. A trapped miscible state was obtained through fast solution casting of film specimens. Time dependence of the structure factor, $S(q,t)$, was measured after the specimen temperature was quickly increased to a final temperature which is above its glass transition temperature, T_g. Thus, the early stage of spinodal decomposition kinetics has been observed starting from the dimension (q^{-1}) comparable to the single chain radius of gyration, R_g, for a binary polymer mixture. The results provide an unequivocal quantitative measure of the virtual structure factor, $S(q,\infty)$; the relationship of q_m and q_c through rate of growth, Cahn-plot analysis, and singularity in $S(q,\infty)$; the growth of fluctuation of $qR_g < 1$ and intrachain relaxation of $qR_g > 1$; and also a clear proof of the Cahn–Hillard–Cook theory in the early stage of spinodal decomposition of a mean-field system.

I. INTRODUCTION

The seemingly simple issue of what is the coexistence curve of a binary mixture of bisphenol-A polycarbonate and poly(methylmethacrylate) (PC/PMMA) has been a long argued problem.[1-9] It was first shown that the DSC, DMS, and cloud point determined coexistence curve seem to depend directly on the thermal heating and the procedure of sample preparation.[5,7,8] The complication is partially due to the crossing or interference of glass transition temperature, T_g, with the coexistence temperature of finite composition for sample preparation and physical measurement.

However, recent time resolved light scattering measurement by Kyu and co-workers[11-13] indicate that the PC/PMMA blend has a lower critical solution temperature (LCST) located well above its corresponding T_g's. Yet, long time annealing experiments by Paul and co-workers[8] indicated that PC/PMMA may have only a very narrow (or no) miscible region above its glass transition temperature line.

One of the possible causes for these conflicting observations could come from the slow kinetics of phase separation due to very low mobility or small thermodynamic driving force for phase separation ($|\partial^2 \Delta F / \partial \phi^2|$, the magnitude of the second derivative of the free energy of mixing) in the system. It could take a long time before composition fluctuations in the system grows to a large enough size and/or amplitude to have sensitivity for DSC, DMS, or cloud point observation. Therefore, a direct examination

of phase separation kinetics at length scales comparable to the single chain dimension ($Rg \sim 50$ Å) is desirable in order to understand the cause of the apparently contradictory observations.[14-16]

In this case, we use small angle neutron scattering (SANS) technique to study a deuterated bisphenol-A polycarbonate/PMMA (dPC/PMMA) blend near and above its T_g to examine the miscibility question. Also, time resolved SANS was used to study the early stage of spinodal decomposition kinetics. By analyzing results according to Cahn–Hilliard–Cook[17,18] theory, details of kinetics as well as thermodynamics can be obtained. It will be shown that it is possible to obtain the phase diagram even though it is buried below the glass transition temperatures. Also, the composition fluctuation growth and single chain relaxation can be studied at different q-regions in the time resolved SANS measurements.

II. EXPERIMENTS

Perdeuterated polycarbonate (dPC) used in this study was synthesized in our laboratory at the NIST. First, the deuterated bisphenol-A was synthesized from phenol-d_6 and acetone-d_6.[19] Then the bisphenol-A is polymerized through condensation polymerization with diphenyl carbonate. The dPC obtained was then fractionated with trichloromethane and methyl alcohol as solvent and nonsolvent pair. Protonated poly(methylmethacrylate) (PMMA) was obtained commercially (Scientific Polymer Product Co.).[20]

The weight-average molecular weights (M_w) were determined by size-exclusion chromatography with light scattering detection as 2.8×10^4, and 3.3×10^4 for dPC and PMMA, respectively. The polydispersity indices (M_w/M_n) estimated from size-exclusion chromatography were 1.4 for dPC, and 2.4 for PMMA. The glass transition temper-

atures (T_g) were measured by differential scanning calorimetry (DSC) as 144 °C for dPC, and 110 °C for PMMA.

Film specimens of dPC/PMMA blend (50/50 wt. %/wt. %) were prepared by dissolving dPC and PMMA in tetrahydrofuran (THF) of $\sim$4 wt. % total polymer concentration. The solution was filtered through a Millipore filter with a pore size of 0.45 μm. A thin film of $\sim$20–40 μm was cast from solution on a thin ($\sim$50 μm) copper sheet at 52 °C. The film was dried in a vacuum oven at 50 °C until it attained to constant weight. The thin, as-cast film thus obtained was cut into 13$\times$13 mm squares, stacked, compressed, and molded at 90 °C into a transparent sample of $\sim$0.5 mm in thickness. These square-shaped specimens were then put between two oxygen-free pure copper disks $\sim$0.2 mm thick with a ring spacer of $\sim$0.5 mm thick.

SANS experiments were carried out at the National Institute of Standards and Technology (NIST) Research Reactor. Pinhole collimation was used with a 9 Å neutron wavelength ($\Delta\lambda/\lambda$=0.25; λ being the wavelength). The observed scattering intensity was corrected for detector and background noise, empty cell scattering, and detector inhomogeneity. The corrected scattering intensity was then converted to an absolute intensity scale with a secondary standard of dry silica gel.[21]

Temperature jump (T-jump) experiments were carried out by manually transferring the specimen, which was kept at 70 °C, onto a copper heating block preheated and controlled at 110 °C$\pm$0.1 °C. Time t=0 was set right after the T-jump. The measuring time varied from 11 to 60 min depending on the scattered intensity level on the two-dimensional detector and the time after temperature jump. Note that the wavelength of the incident neutron was changed from 9 to 12 Å at t=150 min because of the necessity of preventing damage to the detector that would have been caused by the rapidly increasing scattering intensity as phase separation proceeded, and the need of obtaining data at smaller q [$q=(4\pi/\lambda)\sin(\theta/2)$; θ being the scattering angle] range. The SANS profiles measured by the two-dimensional detector were then circularly averaged in order to obtain the dependence on the scattering vector, q.

III. RESULTS AND DISCUSSIONS

For a binary polymer mixture in the miscible region, the static structure factor, $S(q)$, can be described by the random-phase-approximation-calculation.[22] This structure factor, $S(q)$, should be time independent if a true equilibrium has been achieved in the one phase region. In Fig. 1, the structure factor of an as-prepared specimen of the 50/50 dPC/PMMA sample was measured sequentially at 70, 80, 90, and 100 °C using a measurement time of $\sim$1 h each. It can be seen that for 90 and 100 °C the composition fluctuations start to increase. This implies that the seemingly miscible as-prepared blends reflected in the structure factor measured at room temperature are merely in a kinetically "trapped miscible" state. The system will start phase separation as soon as the mobility is increased by raising the temperature to a level near or above the T_g of
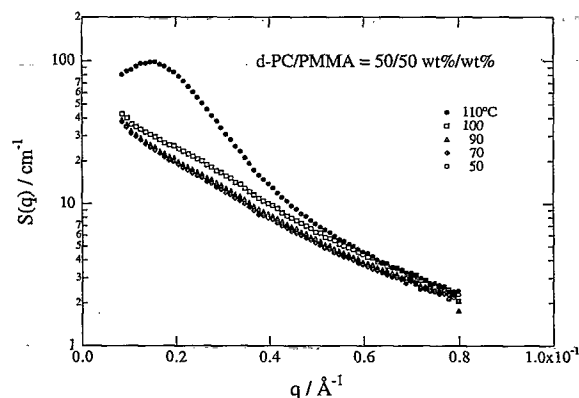

FIG. 1. SANS data from the d-PC/PMMA blend (50/50 wt. %/wt. %) at various temperatures (50, 70, 90, 100, 110 °C) are plotted as $S(q)$ vs q. Measuring time is 1 h for each temperature.

the system. These temperatures (90 and 100 °C) are below the glass transition temperatures of both deuterated polycarbonate and poly(methylmethacrylate); however, the T_g as measured by DSC for this 50/50 as prepared film sample is 86.4 °C which is lower than the T_g of either component for reasons unknown at this time. Two possibilities for this significant change are the presence of residual solvent and the lower T_g of thin films at reduced dimensions.[23] It is unlikely, yet possible, that residual solvent of <0.1 wt. % in this case could lower the T_g from 115 to 86.4 °C. However, this low T_g is not the central issue of this paper, and we will not dwell on this point at this time.

Once we know that this system is only in a kinetically trapped miscible state, we can make a temperature jump to a level where polymer chains have sufficiently high mobility for a real time study at length scales accessible by SANS. In Figs. 2(a) and 2(b), the structure factors $S(q)$, at various times after the temperature jump from 70 to 110 °C are displayed as a function of q. The peak in the structure factor is clearly developed after 22 min. This peak remains at a constant q for $\sim$130 min and then starts to shift toward smaller q. For time <45 min, there may be a slight (not obvious) shift toward smaller q values.[24] All these features typify an early stage of spinodal decomposition up to 130 min and an early to intermediate spinodal decomposition process afterwards.[17]

The early stage of spinodal decomposition kinetics may be described by the Cahn–Hilliard–Cook[17,18] theory, where the time dependent static structure factor, $S(q,t)$, can be written as

$$S(q,t) = S(q,\infty) + [S(q,0) - S(q,\infty)]e^{2R(q)t}, \qquad (1)$$

where $S(q,\infty)$ is the virtual structure factor arising from the introduction of the thermal noise term in the CHC theory and $S(q,0)$ is intensity at t=0. The growth rate $R(q)$ is given as

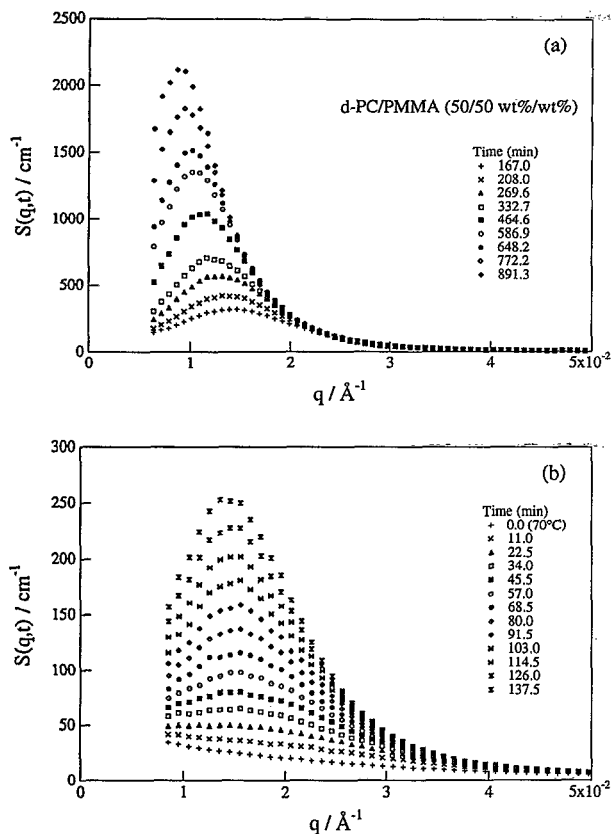$$R(q) = -M(q)q^2\left[\frac{\partial^2\Delta f}{\partial\phi_0^2} + 2\kappa q^2\right], \qquad (2)$$

FIG. 2. Time-evolution of SANS profiles after the temperature jump from 70 to 110 °C. Time elapses in the order of (b) to (a).

FIG. 3. Plot of $\{t/[S(q,t)-S(q,0)]\}^{1/3}$ vs time for temperature jump experiment from 70 to 110 °C at different wave vector q (shown in the graph).

where Δf is the free energy of mixing. Usually the Flory–Huggins function is used for mean-field polymer mixtures to describe Δf, κ is the interfacial free energy density in the Cahn–Hilliard–Cook equation or the Landau free energy expansion, and $M(q)$ is the q-dependent mobility of the binary blend which is normally assumed to be q-independent in the region $qR_g < 1$. The first term on the right-hand side of the Eq. (2) arises from the bulk free energy and the second term from the interfacial free energy.

Equation (1) can be expanded and rearranged[25] into the form

$$\left[\frac{t}{S(q,t)-S(q,0)}\right]^{1/3}$$

$$=\frac{1}{\{2[S(q,0)-S(q,\infty)]R(q)\}}$$

$$\times\left[1-\frac{1}{3}R(q)t+\frac{1}{81}[R(q)t]^3+\cdots\right]. \quad (3)$$

The right-hand side of this equation does not have the second order term in t and can be well approximated by a linear equation in t for $R(q)t < 1$.

In Figs. 3(a) and 3(b), scattering results from Fig. 2 are rearranged and displayed as $\{t/[S(q,t)-S(q,0)]\}^{1/3}$ vs time for the first 8000 s. The solid straight lines are the best fits to the data. From Eq. (3), the ratio of the slope to
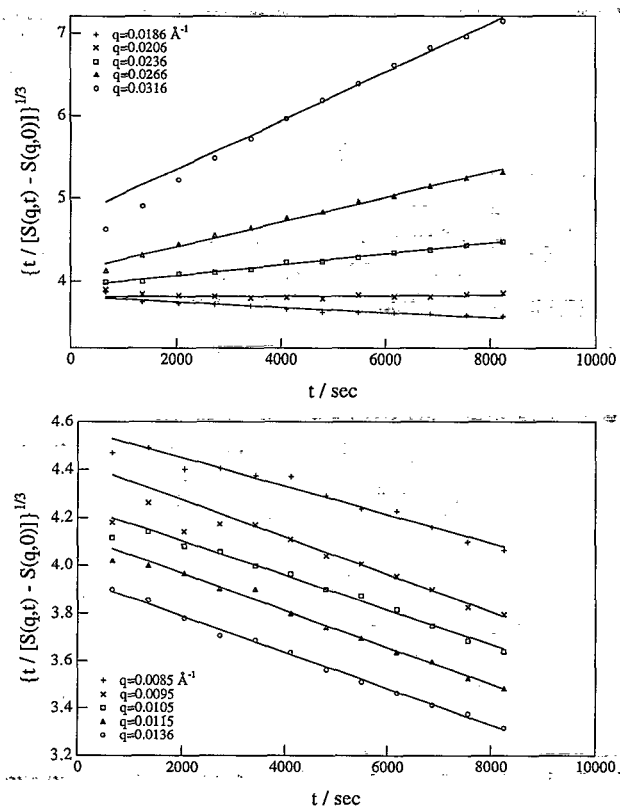
intercept yields the growth (or relaxation) rate of the early stage of the spinodal decomposition. Also the virtual structure factor, $S(q,\infty)$, can be obtained from the intercept. It is interesting to point out that a negative slope yields a positive $R(q)$ at a given scattering wave vector, q. This slope gradually increases and becomes positive for $q > 0.02$ Å^{-1}. This positive slope indicates a negative $R(q)$ which means a relaxation instead of a growth in concentration fluctuation on a length scale (q^{-1}) equal or shorter than the single chain dimension. The rate of growth (or relaxation), $R(q)$, thus obtained is displayed in Fig. 4. $R(q)$ is positive below $q=0.02$ Å^{-1} and has a maximum at $q_m \sim 0.014$ Å^{-1} which corresponds to the maximum in $S(q)$ as shown in Fig. 2. The usual Cahn plot of $R(q)/q^2$ vs q^2 is displayed in Fig. 5. The apparent (or inter) diffusion coefficient, $D_{int}=M\partial^2\Delta f/\partial\phi_0^2$, can be obtained from the intercept as 0.712 (Å^2 s^{-1}). Also in principal the interfacial free energy density, κ, can be obtained if the mobility, M, is known. This will be discussed later. It should be noticed that from Eq. (2) the value of q where the $R(q)$ becomes zero is normally defined as q_c with

$$q_c^2=-\left(\frac{\partial^2\Delta f}{\partial\phi_0^2}\right)\bigg/2\kappa. \quad (4)$$

Also by differentiating $R(q)$ with respect to q in Eq. (2), the q value for the maximum growth rate, q_m, is obtained as
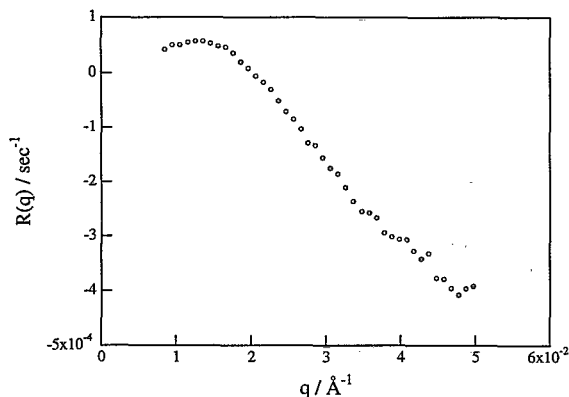
FIG. 4. Plot of growth rate $R(q)$ vs q.

FIG. 6. Virtual structure factor, $S(q,\infty)$ is plotted against q.

$$q_m^2 = -\left(\frac{\partial^2 \Delta f}{\partial \phi_0^2}\right) \Big/ 4\kappa \qquad (5)$$

or

$$q_c^2 = 2q_m^2. \qquad (6)$$

The q_c^2 value of 4×10^{-4} Å^{-2} from Fig. 5 is in complete agreement with $q_m=0.014$ Å^{-1} obtained earlier according to Eq. (6).

The virtual structure factor, $S(q,\infty)$ has been obtained from the intercepts of Fig. 3. This virtual structure factor is displayed in Fig. 6. The virtual structure factor is defined as the structure factor in the two phase region assuming analytical continuity when χ is larger than χ_s ($\chi_s=\chi$ at spinodal point). Where the structure factor can be calculated by RPA as

$$\frac{k_N}{S(q)} = \frac{1}{\phi_A v_A N_A S_A(X_A)} + \frac{1}{\phi_B v_B N_B S_B(X_B)} - \frac{2\chi}{v_0}, \qquad (7)$$
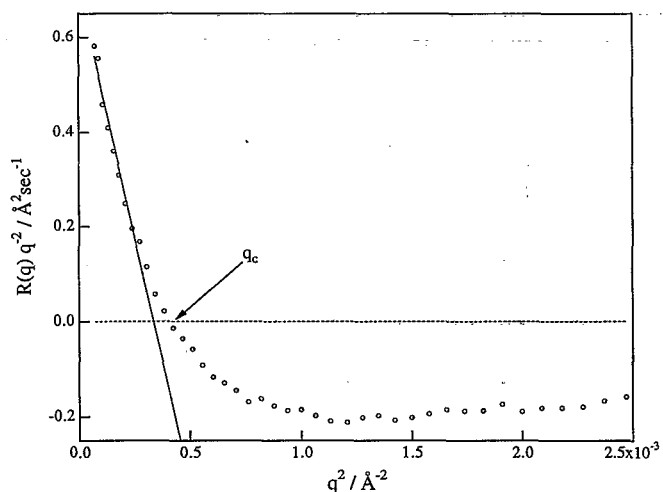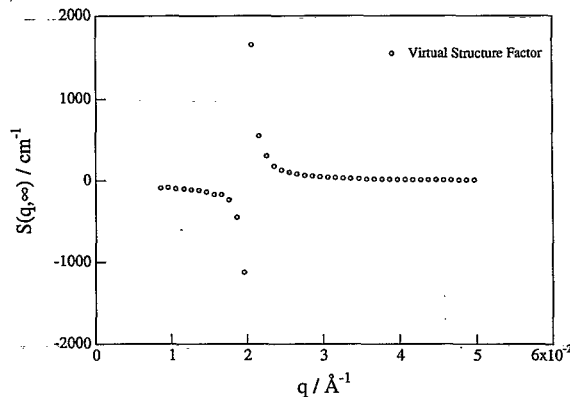

FIG. 5. $R(q) \cdot q^{-2}$ is plotted against q^2 (Cahn plot). The position of q_c is indicated by an arrow in the graph. The interdiffusion coefficient D_{int} was obtained from the intercept of the solid line.

where k_N is the contrast factor, $k_N = N_0 \, (a_A/v_A - a_B/v_B)^2$ with N_0 being the Avogadro number, a_i the scattering length per mole of monomer i, v_0 and v_i being the molar volumes of a reference unit cell and of the ith segment, respectively. The single chain structure factor $S_i(X_i)$ may be represented by the Debye function,

$$S_i(X_i) = 2/X_i^2(e^{-Xi} - 1 + X_i)$$

with $X_i = q^2 R_{gi}^2$ and q is the magnitude of the scattering wave vector

$$q \equiv |\mathbf{q}| = (4\pi/\lambda)\sin(\theta/2),$$

where λ is the wavelength of the incident beam and θ is the scattering angle. R_{gi}, N_i, and ϕ_i are the radius of gyration, the degree of polymerization, and the volume fraction of polymer i, respectively.

With the expansion of the single chain structure factor to the second moment (which should be a valid approximation for $qR_g < 1$ and $R_g^{-1} = 2.12\times10^{-2}$ Å^{-1} in this case), Eq. (7) can be expressed as

$$k_N/S(q) = \frac{1}{N_A \phi_A v_A} + \frac{1}{N_B \phi_B v_B} - \frac{2\chi}{v_0} + \frac{q^2}{3}$$
$$\times \left[\frac{Rg_A^2}{N_A \phi_A v_A} + \frac{Rg_B^2}{N_B \phi_B v_B}\right] \qquad (8)$$

combining with

$$\frac{2\chi_s}{v_0} = \frac{1}{N_A \phi_A v_A} + \frac{1}{N_B \phi_B v_B}, \qquad (9)$$

$$\frac{\partial^2 \Delta f}{\partial \phi_0^2} = k_B T \left[\frac{2}{v_0}(\chi_s - \chi)\right], \qquad (10)$$

and

$$\kappa = \frac{k_B T}{6}\left[\frac{Rg_A^2}{\phi_A N_A v_A} + \frac{Rg_B^2}{\phi_B N_B v_B}\right], \qquad (11)$$

then

$$\frac{k_N}{S(q)} = \frac{1}{k_B T}\left[\frac{\partial^2 \Delta f}{\partial \phi_0^2} + 2\kappa q^2\right]. \qquad (12)$$
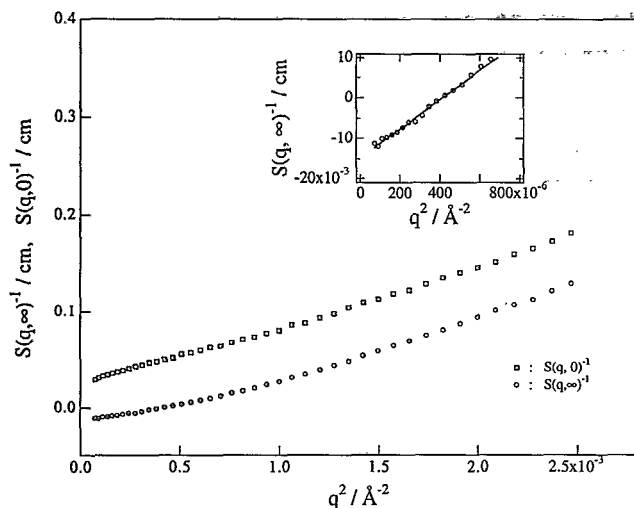
FIG. 7. Reciprocal virtual structure factor, $S(q,\infty)_{-1}$, and reciprocal initial structure, $S(q,0)^{-1}$ are plotted against q^2. The inserted figure shows the $S\infty (q)^{-1}$ vs q^2 at small q ($0 < q(\text{Å}^{-1}) < 0.028$). $\chi/v0$ at 110 °C for d-PC/PMMA blend was obtained from the intercept of the line in the inserted figure.

Again, $S(q)$ should diverge at $q^2 = -(\partial^2\Delta f/\partial\phi_0^2)/2\kappa = q_c^2$. The experimental value of $q_c = 2\times10^{-2}$ Å^{-1} from Fig. 6 is identical to that obtained earlier from Fig. 5.

Since we have assumed the analytical continuity of χ as a function of temperature across the phase boundary, the inverse plot of the virtual structure factor, i.e., $S(q,\infty)^{-1}$ vs q^2 should be parallel to that in the one phase region, since the virtual structure factor is defined as the structure factor of a blend that is instantaneously brought from the miscible region to immiscible region and then reaches the final temperature before any change in the spatial distribution of polymer chains. This temperature change gives a new $\chi(T)$ which is larger than χ_s. Since the chain distribution was not changed, therefore it is clear from either Eq. (7) or Eq. (8) that an inverse plot of the structure factor $S(q)^{-1}$ vs q^2 should give a series of parallel lines. This is demonstrated in Fig. 7.

The intercept of $S(q,\infty)^{-1}$ vs q^2 plot should give the value of χ/v_0 in the two phase region. This χ/v_0 value obtained for $T=110$ °C is 1.13×10^{-4}.

We should mention at this point that the specimen was prepared by solution casting. A trapped miscible state is obtained through fast solvent evaporation. The duplication of this condition is very important even though the rate of growth, $R(q)$ in the CHC analysis of the linear kinetics of spinodal decomposition is assumed to be independent of the initial condition, $S(q,0)$. We did repeat our experiment for the whole analysis as discussed above. For two separate preparations $S(q,0)$ is slightly different which reflects the differences in evaporation processes. However, the final results of $S(q,\infty)$ and χ are well within the experimental uncertainties of each other. The q_m and q_c obtained are identical within experimental error for the two preparations. However the $R(q)$ values are somewhat different, which probably reflects the influence of the initial state that linear theory of CHC type does not include.[26]

IV. CONCLUSION

It is obvious from our time resolved SANS study that 50/50 blend of dPC/PMMA is immiscible above its glass transition temperature. A trapped miscible state can be obtained through fast solution casting of thin film (~50 μm) in THF. A slow spinodal kinetics has been studied by SANS by heating the solvent cast specimen to a temperature above its T_g, meanwhile the mobility, M, of the interdiffusion is still slow enough to keep the interdiffusion coefficient, D_{int} ($D_{\text{int}}=M\partial^2\Delta f/\partial\phi_0^2$) small enough for the time resolved SANS study.

Because the SANS experiment covers a q-range which encompasses the single chain dimension, i.e., from $qR_g > 1$ and $qR_g < 1$, the time dependent structure factor thus obtained provides unequivocal quantitative measure of the virtual structure factor, $S(q,\infty)$; the relationship of q_m and q_c through $R(q)$, Cahn-plot analysis and singularity in $S(q,\infty)$; the growth of fluctuation at $qR_g < 1$ and intrachain relaxation at $qR_g > 1$; and finally a clear proof of CHC theory in the very early stage of spinodal decomposition.

We have used a q-independent mobility, M, for the above analysis. A more detailed analysis of including single chain dynamics in the q-dependent mobility, $M(q)$ such as the Rouse dynamics of Binder[27] or reptation dynamics of Pincus[28] is underway. Our initial results indicate that these analysis do not change the results presented in this paper which is focused on the region of $qR_g < 1$.

We should also point out that this procedure provided a technique of obtaining the functional form of the free energy of mixing of immiscible blends by measuring the temperature dependence of χ parameters at various compositions and final temperatures through measurements of the kinetics of spinodal decomposition. The phase diagram which is inaccessible due to the interference of T_g line, can be obtained through temperature extrapolation of χ parameter. The intrachain relaxation can in principle be studied from the time and q dependence of $S(q)$ in the region of $qR_g > 1$. These analyses are currently underway.

[1] Z. G. Garlund, Poly. Prep. Am. Chem. Soc. Div. Polym. Chem. **23**, 258 (1982).
[2] Z. G. Garlund, Adv. Chem. Ser. No. 206, 129 (1984).
[3] K. K. Koo, T. Inoue, and K. Miyasaka, Polym. Eng. Sci. **27**, 741 (1985).
[4] T. Kyu and J. M. Saldanha, J. Polym. Sci. Polym. Lett. Ed. **26**, 33 (1985).
[5] J. M. Saldanha and T. Kyu, Macromolecules **20**, 2840 (1987).
[6] T. Kyu and D. S. Lim, J. Polym. Sci. Polym. Lett. **27**, 421 (1989).
[7] J. S. Chion, J. W. Barlow, and D. R. Paul, J. Polym. Sci. Phys. Ed. **25**, 1459 (1987).
[8] M. Nishimoto, H. Keskkula, and D. R. Paul, Polymer **32**, 272 (1991).
[9] R. P. Kambour, P. E. Gundlack, I. C. W. Wang, D. M. White, and D. W. Yeager, Am. Chem. Soc. Div. Polym. Sci. Polym. Prepr. **28-2**, 140 (1987).
[10] D. R. Paul and S. Newman, *Polymer Blends* (Academic, New York, 1978).
[11] T. Kyu and J. M. Saldanha, Macromolecules **21**, 1021 (1988).
[12] P. S. Lim and T. J. Kyu, Chem. Phys. **92**, 3944 (1990).
[13] T. Kyu and D. S. Lim, J. Chem. Phys. **92**, 3951 (1990).
[14] G. R. Strobl, Macromolecules **18**, 558 (1985).
[15] J. S. Higgins, H. Fruitwala, and P. E. Tomlins, Macromolecules **23**, 3674 (1989).
[16] D. Schwahn, S. Jansen, and T. Springer, J. Chem. Phys. **97**, 8775 (1993).

[17] J. W. Cahn and J. E. Hilliard, J. Chem. Phys. **31**, 688 (1959); J. W. Cahn, *ibid.* **42**, 93 (1965).

[18] H. E. Cook, Acta Metall. **18**, 297 (1970).

[19] W. L. Wu and B. J. Bauer, Polym. Commun. **26**, 39 (1985).

[20] Certain commercial materials and equipment are identified in this paper in order to specify adequately the experimental procedure. In no case does such identification imply recommendation or endorsement by the National Institute of Standards and Technology nor does it imply that the material or equipment identified is necessarily the best available for this purpose.

[21] C. J. Glinka, J. M. Rowe, and J. G. LaRock, J. Appl. Crystallogr. **19**, 427 (1986).

[22] P.-G. de Gennes, *Scaling Concept in Polymer Physics* (Cornell University, Ithaca, 1979); J. Chem. Phys. **72**, 4756 (1980).

[23] C. L. Jackson and G. B. McKenna, J. Non-Cryst. Solid **131–133**, 221 (1991).

[24] This apparent shift of q_m at very early time of spinodal decomposition is due to the time independent first term, $S(q,\infty)$ in Eq. (1). Once the scattering intensity is dominated by the second term in Eq. (1), the peak position becomes constant in the early stage of S.D.

[25] T. Sato and C. C. Han, J. Chem. Phys. **88**, 2057 (1988).

[26] A. Z. Akcasu, I. Bahar, B. Erman, Y. Feng, and C. C. Han, J. Chem. Phys. **97**, 5782 (1992).

[27] K. Binder, J. Chem. Phys. **63**, 6387 (1983).

[28] P. Pincus, J. Chem. Phys. **75**, 1996 (1981).